Theoretical investigation of weakly-bound complexes of O (3 P) with H 2

Millard H. Alexander

Citation: The Journal of Chemical Physics **108**, 4467 (1998); doi: 10.1063/1.475858
View online: http://dx.doi.org/10.1063/1.475858
View Table of Contents: http://scitation.aip.org/content/aip/journal/jcp/108/11?ver=pdfcov
Published by the AIP Publishing

Theoretical investigation of weakly-bound complexes of $O(^3P)$ with H_2

Millard H. Alexander
Department of Chemistry and Biochemistry, University of Maryland, College Park, Maryland 20742-2021

(Received 7 October 1997; accepted 15 December 1997)

We report multireference configuration interaction (CI), as well as coupled-cluster, calculations for the three $O(^3P)H_2$ potential-energy surfaces (two of A'' symmetry and one of A' symmetry in C_s geometry) in the region relevant to the weakly bound $O(^3P)\cdots H_2$ complex. The two electronically adiabatic states of A'' symmetry correspond to an orthogonal transformation of two orthogonal electronic occupations of the O $2p$ orbitals. The transformation of the three electronically adiabatic states to an approximate diabatic representation, which involves four potential-energy functions, can be obtained, either from calculated matrix elements of the electronic orbital angular momentum or from analysis of the expansion coefficients of the CI wave functions. An exact treatment of the nuclear motion including spin–orbit coupling, based on the diabatic PES's (potential energy surfaces), is used to determine the energies of the lowest bend–stretch levels of complexes of $O(^3P)$ with both nuclear spin isomers of H_2 and D_2. The predicted dissociation energies (D_0) are 15.4 and 22.4 cm^{-1} for the complexes with pH_2 and oH_2, respectively, and 22.3 and 31.4 cm^{-1} for the complexes with oD_2 and pD_2, respectively. © *1998 American Institute of Physics.*
[S0021-9606(98)02111-4]

I. INTRODUCTION

For many years the $O(^3P)+H_2$ system has been the object of theoretical study, motivated, no doubt, by the importance of the $O(^3P)+H_2\rightarrow OH+H$ reaction in combustion.[1] Howard, McLean, and Lester presented an early, informative, *ab initio* study of the relevant potential-energy surfaces.[2] More complete *ab initio* calculations were reported by Walch and co-workers.[2] Their potential-energy surfaces underlie numerous subsequent theoretical investigations of the reactive dynamics by Schatz, Bowman, and Wagner and their co-workers.[3–5] The reaction of $O(^3P)$ with H_2 has a high barrier. The minimum barrier ($\sim$13.5 kcal/mol[6]) occurs in linear geometry, and corresponds to a $^3\Pi$ electronic state, in which three of the four O2p electrons occupy orbitals which are perpendicular to the O–H_2 axis.

Because of this high barrier to reaction it may be possible to stabilize ground-state oxygen atoms in liquid or solid H_2. For this reason, doping of atomic O into solid H_2 has been suggested as a possible pathway to enhancing the specific impulse of cryogenic propellants.[7] Motivated by this suggestion, Li, Apkarian, and Harding (LAH) recently presented[8] a new *ab initio* investigation of the $O(^3P)H_2$ PES's in the region of the van der Waals minimum. They predicted a well depth greater than 100 cm^{-1}. In their subsequent investigation of the structure of the binary $O(^3P)\cdots H_2$ complex, LAH treated only the p-H_2 nuclear spin modification as well as neglecting the spin–orbit splitting of the O atom. An adiabatic model was used to simulate the O–H_2 stretching motion. Within these approximations, LAH predicted a zero-point corrected dissociation energy D_0 of $\sim$50 cm^{-1}.

In our earlier investigation[9,10] of the similar calculations on the $B(^2P)\cdots H_2$ complex, agreement with the experimental laser-excited fluorescence spectrum[11] of this complex depended critically on the proper treatment of (a) the mixing between the three PES's which arise from the threefold degeneracy of the $2p$ orbital and (b) the role of the spin–orbit coupling in the B atom, which is comparable to the splitting between these PES's. In addition, as in all weakly bound complexes, the nuclear motion is too anharmonic, and the well depths too small, for a harmonic approximation to give a reliable estimate of the zero-point correction to the dissociation energy.

The two $O(^3P)H_2$ electronic states of antisymmetric (A'') reflection symmetry, represent, in the simplest picture, an orthogonal transformation of two orthogonal assignments of the four O $2p$ electrons: $p_x^2p_yp_z$ and $p_xp_yp_z^2$. The third state, the sole of A' reflection symmetry, corresponds to the third possible assignment: $p_xp_y^2p_z$. Here the y axis is perpendicular to the plane of the triatomic. As in the case of $B(^2P)\cdots H_2$, in a treatment of the nuclear motion of the $O(^3P)+H_2$ system it is most convenient to use an electronically diabatic representation, in which the three states are so described and where the axis system is defined with respect to the vector R which joins the atom to the center-of-mass of the H_2 molecule.[9,12,13]

In our work on $B(^2P)\cdots H_2$,[9] we followed the pioneering work of Rebentrost and Lester[14] on the $F(^2P)+H_2$ system and used the matrix elements of the electronic orbital angular momentum $\mathbf{l}$ to define the approximate adiabatic→diabatic transformation. Alternatively, one can use the CI coefficients of the dominant configurations to define the adiabatic→diabatic transformation.[10,15] We have applied the same methods here to determine the diabatic $O(^3P)H_2$ PES's. As will be seen below, the two transformations so obtained are almost equivalent. In addition, both transformations predict derivative coupling matrix elements which are nearly identical to those calculated numerically, directly from the adiabatic electronic wave functions. Our *ab*

initio calculations (discussed in Sec. II), although more extensive than those of LAH, yield well depths which are considerable less than found by these authors.

Using our diabatic $O(^3P)H_2$ PES's,[9] we then predict the energies and structures of the lowest bend–stretch levels of the complex of $O(^3P)$ with H_2 and D_2. To do so, we make use of the general treatment by Dubernet and Hutson[13] of complexes between open-shell atoms and closed-shell diatomic molecules. We shall report on the results of these calculations in Secs. III and IV below. The zero-point corrected dissociation energies (15.4 and 22.4 cm^{-1} for the complexes with pH_2 and oH_2, respectively, and 22.3 and 31.4 cm^{-1} for the complexes with oD_2 and pD_2, respectively) are substantially smaller than the earlier estimates.[8]

II. AB INITIO INVESTIGATIONS

A. Methods

We here use complete active space, self-consistent field (CASSCF)[16] calculations, supplemented by multireference, configuration interaction (MRCI) calculations, to determine the $O(^3P)H_2$ PES's. In exploratory calculations we used the augmented, correlation-consistent, valence-triple-zeta ($avtz$) atomic orbital basis of Dunning and co-workers[17,18] ($11s6p3d2f$ contracted to $5s4p3d2f$ for O and $6s3p2d$ contracted to $4s3p2d$ for H). For determination of the full PES's we used the larger quadruple-zeta basis ($avqz$)[17,18] ($13s7p4d3f2g$ contracted to $6s5p4d3f2g$ for O and $7s4p3d2f$ contracted to $5s4p3d2f$ for H). To describe the active spaces in our CASSCF calculations we shall use the notation[19] (nmm/kl). Here n and m are the number of occupied σ and π orbitals, respectively, of which the lowest $k\sigma$ and $l\pi$ orbitals are maintained closed (inactive) in the reference wave function. Full valence CASSCF calculations (511/1) were done, in which the reference configurations were generated by distributing eight electrons among the seven valence orbitals. State averaging was used to determine the CASSCF orbitals; equal weights were assigned to the three states which arise when $O(^3P)$ approaches a closed-shell molecular partner. At large values of the O–H_2 distance, some difficulties were encountered in maintaining smooth values of the interaction potential. This arises because the nominal CASSCF $1s$ orbitals on the O end up containing some small fraction of $2s$ character. Since the $1s$ orbital is not correlated in the resulting CI, this can cause slight irregularities in the calculated CI potential. We found that this difficulty could be eliminated by requiring the $2s$ orbital to remain doubly filled in the CASSCF calculation (511/2).

The contribution of higher-order excitations which are not explicitly included in the multireference configuration interaction can be estimated with the internally contracted, multireference version[20] of the Davidson correction (MRCI+Q).[21,22] All calculations were carried out with the MOLPRO suite of *ab initio* programs.[23]

The OH_2 system will be described by the usual Jacobi coordinates, R, r, and θ. In most of the calculations to be presented here, the H_2 molecule was kept at its equilibrium bond distance {1.402 bohr in coupled cluster [CCSD(T)] calculations[24,25] with the $avqz$ basis}. Asymptotically, without loss of generality one can choose the three degenerate states of the O atom in its ^3P electronic ground state to correspond to the following three orbital occupations introduced in Sec. I: $p_x^2p_yp_z(P_{x^2})$, $p_xp_y^2p_z(P_{y^2})$, and $p_xp_yp_z^2(P_{z^2})$. We take the z axis to lie along **R**, the x axis to be perpendicular to **R** but still in the triatomic plane, and the y axis to be perpendicular both to **R** and to the triatomic plane.

In C_{2v} geometry each of these three orbital occupations belongs to a different point group (b_1 for P_{x^2}, b_2 for P_{y^2}, and a_2 for P_{z^2}). In $C_{\infty v}$ geometry, there exist two distinct orientations: Π (P_{x^2} and P_{y^2}) and $\Sigma^-(P_{z^2})$. Except in these high symmetry cases, the P_{x^2} and P_{z^2} configurations are of a'' symmetry while the P_{y^2} configuration is of a' symmetry. The interaction energy for each state, and at each geometry, is defined as

$$V(R,r,\theta)=E_{O-H_2}(R,r,\theta)-E_{H_2}(R,r,\theta) - E_O(R,r,\theta)-\Delta E_{SC}. \quad (1)$$

Here, $E_{H_2}(R,r,\theta)$ and $E_O(R,r,\theta)$ are the calculated energies of the separate fragments but in the supermolecule atomic orbital basis and ΔE_{SC} is the correction for the residual size consistency of the calculations

$$\Delta E_{SC}=E_{O-H_2}(\infty)-E_{H_2}(\infty)-E_O(\infty). \quad (2)$$

The subtraction, in Eq. (1), of the energies of the separate fragments in the supermolecule basis constitutes the counterpoise correction,[26] which corrects for the lack of saturation of the atomic orbital basis,

For the higher symmetry geometries ($C_{\infty v}$ and C_{2v}), the accuracy of the calculated potentials can be assessed by comparison with coupled-cluster calculations [UCCSD(T)],[24,25] in which all single- and double-excitations out of a single-reference unrestricted Hartree–Fock wave function are included, as well as the contribution of triple excitations, determined perturbatively. Figure 1 displays the calculated collinear ($C_{\infty v}$) and perpendicular (C_{2v}) $O(^3P)H_2$ interaction energies in the region of the van der Waals minimum. The well depths and equilibrium bond lengths are given in Table I.

The $^3A_2$ potential ($^3\Sigma^-$ in collinear geometry) is least attractive in perpendicular geometry, since in this state the O $2p_z$ orbital, which points directly at the H_2 bond, is doubly filled and hence undergoes the largest degree of Pauli repulsion with the filled H_2 bonding orbital. In collinear geometry, however, the $^3\Sigma^-$ state is the most attractive. This is likely a result of the more favorable interaction between the quadrupole moment of the H_2 molecule (positive at the ends and negative in the middle) and the quadrupole moment of the O atom, which is most negative in the direction of the doubly filled $2p$ orbital. The magnitudes of the wells in the other two states are, however, comparable for both geometries. In perpendicular geometry, the $^3B_1(P_{x^2})$ state lies slightly lower than the $^3B_2(P_{y^2})$ state. In the former the doubly occupied $2p$ orbital lies in the molecular plane, and hence the singlet-coupled pair of O $2p$ electrons can use the unoccupied σ^*H_2 orbital to correlate.

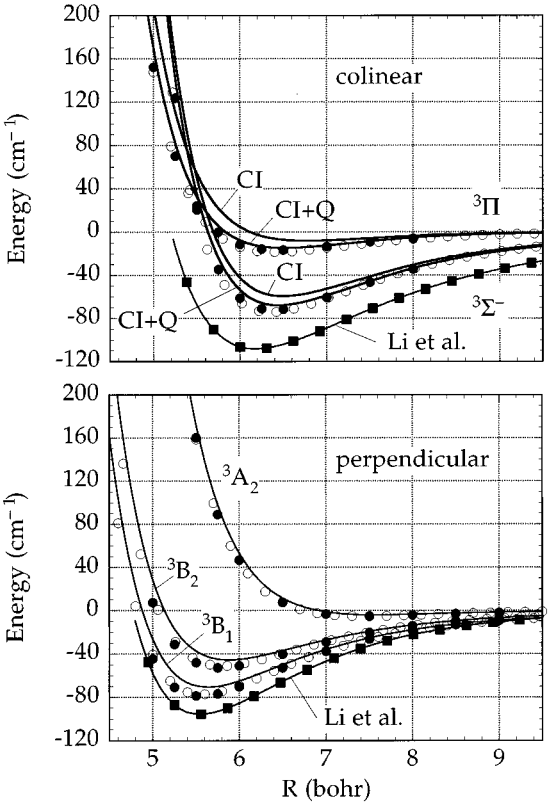

FIG. 1. (Upper panel) Comparison of calculated potential-energy curves for the $^3\Sigma^-$ and $^3\Pi$ curves of the O(^3P)H_2 complex in collinear ($C_{\infty v}$, upper panel) and perpendicular (C_{2v}, lower panel) geometries. In both panels the MRCI+Q interaction energies are shown with solid curves, the CCSD(T) energies are shown with filled circles, and the scaled external correlation energies with $s=1.21$ are shown with open circles. In addition, in the upper panel, the MRCI energies are also shown with solid curves. All these calculations were carried out with $avqz$ atomic orbital bases. The position and depth of the minima for each curve are listed in Table I. For comparison, in both panels, the filled squares indicate the lowest energy potential curve of Li *et al.* (Ref. 8), determined with an $avtz$ orbital basis and a different configuration interaction method.

The UCCSD(T) curves have substantially deeper wells, because the inclusion of triple excitations allows for a more complete recovery of the correlation energy which is responsible for the dispersion forces which provide a large fraction of the binding in any van der Waals molecule. To compensate for this incomplete recovery of the correlation energy, in previous work[27,28] on other weakly bound species, and following earlier suggestions by several groups,[29,30] we have augmented the calculated external correlation energy. We define a scaled external correlation (SEC) interaction energy by introduction of a parameter s, as follows;

$$V_{\rm sec}(R,\theta)=V_{\rm CASSCF}(R,\theta)+s\times V_{\rm CORR}(R,\theta), \tag{3}$$

where $V_{\rm CORR}$ is defined as the difference between the CASSCF and MRCI interaction energies

$$V_{\rm CORR}(R,\theta)=V_{\rm MRCI}(R,\theta)-V_{\rm CASSCF}(R,\theta). \tag{4}$$

For brevity we suppress, except where explicitly necessary, the dependence on the H_2 bond distance r. The scaling factor s is independent of geometry. The MRCI interaction energies correspond to a scaling factor of unity.

TABLE I. Calculated values of R_e and D_e for colinear and perpendicular arrangements of the O(^3P)$\cdots H_2$ complex.[a]

Method	R_e (bohr)	D_e (cm^{-1})
	Collinear $^3\Pi$	
MRCI ($s=1$)	6.77	8.1
MRCI+Q[b]	6.49	14.3
MRCI ($s=1.21$)[c]	6.38	18.3
CCSD(T)	6.39	16.5
	Collinear $^3\Sigma^-$	
MRCI ($s=1$)	6.47	59.3
MRCI+Q[b]	6.42	67.9
MRCI ($s=1.21$)[c]	6.34	74.4
CCSD(T)	6.39	72.0
MRCI+Q[d]	6.18	108.3
	Perpendicular $^3B_1$	
MRCI ($s=1$)	5.77	56.4
MRCI+Q[b]	5.62	70.2
MRCI ($s=1.21$)[c]	5.55	76.9
CCSD(T)	5.56	78.9
MRCI+Q[d]	5.54	95.5
	Perpendicular $^3A_2$	
MRCI ($s=1$)	7.69	2.1
MRCI+Q[b]	7.55	4.4
MRCI ($s=1.21$)[c]	7.46	5.6
CCSD(T)	7.44	5.0
	Perpendicular $^3B_2$	
MRCI ($s=1$)	6.00	35.2
MRCI+Q[b]	5.86	45.8
MRCI ($s=1.21$)[c]	5.80	51.2
CCSD(T)	5.55	52.7

[a]All calculations use the $avqz$ basis of Dunning and co-workers (Refs. 17 and 18) except where explicitly stated.
[b]See Ref. 22.
[c]Scaled external correlation correction; see Eq. (3).
[d]Reference 8; calculations with the $avtz$ basis of Refs. 17 and 18.

We see in Fig. 1 that a scaling factor of $s=1.21$ reproduces extremely well the UCCSD(T) interaction energies, slightly underestimating the well depth in colinear geometry but slightly overestimating the well depth in perpendicular geometry. Accordingly, we used this scaling factor in the determination of the PES's at all geometries. Calculations were carried out at 12 values of R (3.5:0.5:7, 8, 9, 10, and 12 bohr) and nine values of θ equally spaced between 0 and $\pi/2$. The size consistency corrections, evaluated at $R=30$ bohr, were 464.7 and 466.9 cm^{-1} for the $avqz$ MRCI calculations on the A' and A'' states, respectively (both A'' states had identical SC corrections). For the MRCI+Q calculations, these values dropped to 21.5 and 23.0 cm^{-1}, respectively.

In the bulk of the calculations we kept the H_2 bond distance frozen at the equilibrium value in the isolated molecule (1.402 bohr). To confirm the validity of this calculation we carried out some additional UCCSD(T) calculations for both colinear and perpendicular geometry at several values of R which sample the inner wall of the potential, but still in the region of the minimum. The results of these calculations are shown in Fig. 2. At least at these values of the O–H_2 distance, approach of the O atom causes very little, if any, distortion of the H_2 bond. Thus, the use here of a frozen H_2 bond is justified.

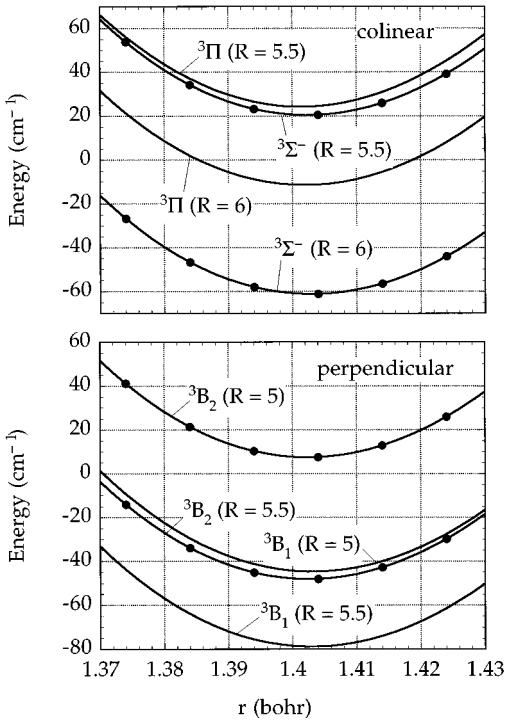

FIG. 2. The dependence on r, the H_2 bond length, of the PES's of the $O(^3P)H_2$ complex for colinear (upper panel, Π and Σ^- PES's) and perpendicular (lower panel, B_1 and B_2 PES's) geometries, determined with UCCSD(T) calculations with the $avqz$ basis. The potential curves are shown for two values of R (5.5 and 6 bohr for colinear and 5 and 5.5 bohr for perpendicular), which correspond (Fig. 1) to distances which sample the inner wall of the potential, but still in the region of the minimum. The CI equilibrium bond length of the isolated H_2 molecule is 1.402 bohr. The A_2 PES, not shown in the lower panel, is quite repulsive at these values of R. Notwithstanding, the dependence on r also shows a minima at $r \cong 1.402$ bohr.

B. Determination of the adiabatic+diabatic transformation

In arbitrary C_s geometries, as the O atom approaches the H_2 molecule, the lowest two adiabatic states of A'' symmetry represent, to a good approximation, a 2×2 orthogonal transformation of the two, asymptotically degenerate, diabatic states of A'' symmetry (P_{x^2} and P_{z^2}). This transformation can be represented by a single transformation angle $\gamma(R,r,\theta)$, as follows:

$$\begin{bmatrix} 1A' \\ 2A' \end{bmatrix} = \begin{bmatrix} \cos\gamma & \sin\gamma \\ -\sin\gamma & \cos\gamma \end{bmatrix} \begin{bmatrix} P_{x^2} \\ P_{z^2} \end{bmatrix}. \tag{5}$$

The angle γ also corresponds to an orthogonal rotation, in coordinate space, of the $p_{x^2}p_z$ and $p_xp_{z^2}$ configurations. The magnitude of this rotation depends on the position of the H_2 molecule. For perpendicular (C_{2v}) geometry the A_2 state (P_{z^2}) always lies above the B_1 state (P_{x^2}), so that the rotation angle in Eq. (5) is always 0°. For linear geometry the angle γ is 90° at long range, where the Σ^- state (P_{z^2}) lies below the Π state (P_{x^2}), but switches to 0° at shorter range, where the Π state crosses below the Σ^- state.[9]

Because of the high barriers on the $O(^3P)H_2$ potential-energy surfaces,[2,6,7] the van der Waals interaction of $O(^3P)$ with H_2 will not involve bond formation. Consequently, the orthogonal rotation of the two configuration state functions corresponding to $O(P_{z^2})H_2$ and $O(P_{x^2})H_2$ will be well mirrored by the matrix of the x (or z) component of the electronic orbital angular momentum $\mathbf{l}$.[9,14] Accordingly, following the original suggestion of Rebentrost and Lester,[14] we propose[9]

$$\gamma = \tan^{-1}\langle 1A''|l_x|1A'\rangle / \langle 2A''|l_x|1A'\rangle. \tag{6}$$

Here the states $|1A''\rangle$ and $|2A''\rangle$ designate, respectively, the wave functions for the upper and lower electronically adiabatic states of A'' symmetry, and $|1A'\rangle$ designates the wave function for the sole state of A' symmetry [$O(P_{y^2})H_2$].

An alternative approach to the determination of the adiabatic→diabatic transformation, proposed some years ago by Werner and co-workers,[15] is to assume that the transformation angle is given by

$$\gamma = \cos^{-1}\left[C^{1A''}_{P_{x^2}} \Big/ \sum_i C_i^2 \right], \tag{7}$$

Where C_i denotes the coefficient of the ith configuration state function (csf) in the MRCI wave function and $C^{1A''}_{P_{x^2}}$ is the coefficient in the $|1A''\rangle$ state of the csf with electron occupancy $(1a')^2(2a')^2(3a')^24a'^25a'1a''$. Here the $1a'$ and $2a'$ orbitals correspond to the O $1s$ and $2s$ orbitals, the $3a'$ orbital corresponds to the $H_2 1\sigma_g$ orbital, and the $4a'$, $5a'$, and $1a''$ orbitals correspond, respectively, to the O $2p_x$, $2p_z$, and $2p_y$ orbitals.

For consistency in applying this method, we must ensure that the information on the 2×2 rotation of the O P_{z^2} and P_{z^2} configurations is contained in the CI coefficients, rather than in the CASSCF orbitals. To do so, after each CASSCF calculation, at any arbitrary geometry, we rotate the orbitals of the $1A''$ and $2A''$ wave functions to attain maximum overlap with the comparable orbitals at a reference geometry (R and r unchanged) where there is no $P_{x^2}-P_{z^2}$ mixing.[15] In the case of OH_2 this reference geometry could be either colinear or perpendicular. Here we used a colinear reference geometry, since a conical intersection occurs in colinear geometry.

The upper panel of Fig. 1 reveals that for $r = 1.402$ bohr this conical intersection occurs in linear geometry at $R\sim5.5$ bohr. The upper panel of Fig. 3 displays the dependence on θ, the bending angle, of the diabatic and adiabatic $O(^3P)H_2$ PES's in the neighborhood of this conical intersection. The middle panel of Fig. 3 compares the transformation angle calculated by Eqs. (6) and (7). As can be seen, both methods agree extremely well.

Nonetheless, these diabatic transformations are only approximate. A measure of their accuracy is a comparison of the derivative of the transformation angle and the corresponding off-diagonal derivative matrix element, in the adiabatic basis. These will be equal for the true diabatic transformation, so that

$$\partial\gamma/\partial q = \langle 1A''|\partial/\partial q|2A'\rangle, \tag{8}$$

where q designates any nuclear coordinate (R, r, or θ). The lower panel of Fig. 3 compares the derivative of the trans-

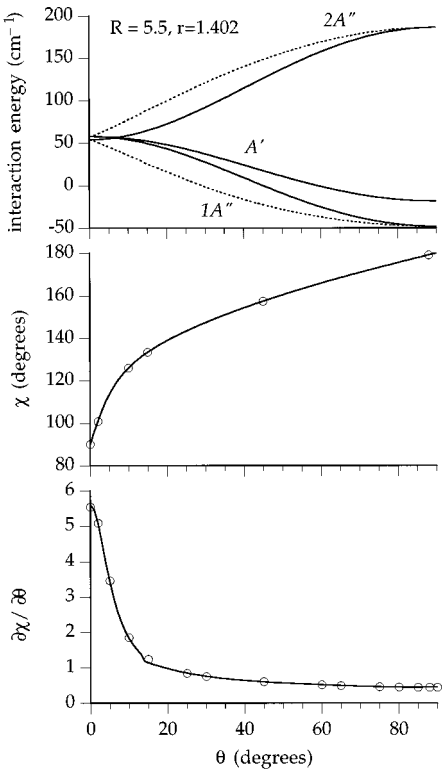

FIG. 3. (Upper panel) Comparison of the dependence on θ of the electronically diabatic (solid curves) and adiabatic (dashed curves) $O(^3P)H_2$ potentials for $R=5.5$ bohr, and $r=1.402$ bohr, determined from MRCI calculations with the $avtz$ basis sets. For this value of r the conical intersection occurs at $R=5.48$ bohr. The adiabatic potential curves are shown only for the two states of A'' symmetry, since the diabatic and adiabatic curves are identical for the unique state of A' symmetry. (Middle panel) Dependence on θ of the diabatic transformation angle, from the same calculations with the $avtz$ basis set. The solid curves were extracted from the l_z matrix elements in the electronically adiabatic basis. The open circles indicate values obtained from the CI coefficients (Eq. 7). (Lower panel) The dependence on θ of the derivative of the diabatic transformation angle shown in the middle panel (solid curves) compared with the calculated derivative coupling matrix elements $\langle 1A''|\partial/\partial\theta|2A''\rangle$.

formation angle, with respect to θ, obtained from Eq. (6), with the corresponding derivative coupling matrix element. The agreement is near perfect, which confirms the accuracy of our method for transforming into an electronically diabatic representation.

For C_s geometry it is difficult to apply, in a consistent manner, a counterpoise correction to the calculated electronically adiabatic energies of the two states of A'' symmetry. At many geometries the upper, more repulsive of the two A'' surfaces will correspond to the $O(P_{z^2})$ orbital occupation, where the $2p_z$ orbital which points toward the H_2 is doubly filled. However, in the counterpoise calculations for the O atom, the lower of the A'' states may correspond to this same orbital occupation, since in this orientation the ghost H_2 orbitals can be used to greatest advantage to correlate the electrons of the O atom. Thus, it is difficult to predict, independent of geometry, which of the two O atom A'' energies should be used in the counterpoise correction for a given OH_2 state of A'' symmetry.

In our calculations we first transform the $O(^3P)H_2$ energies, as well as the $O(^3P)$ energies determined with the full (supermolecule) basis, into the diabatic basis before making the counterpoise correction. Of course, for the unique state of A' symmetry, as well as for the H_2 fragment, the diabatic and adiabatic states are identical. Diabatic potential-energy surfaces were obtained at both the CASSCF and MRCI level. Subsequently, the diabatic SEC potential-energy surfaces were determined from Eq. (3) with a scaling factor of $s=1.21$.

C. Comparison with previous calculations

As mentioned in the Introduction, Li, Apkarian, and Harding (LAH) have already published[8] an extensive MRCI investigation of the $O(^3P)H_2$ PES's in the region of the van der Waals minimum. These authors used the smaller $avtz$ basis, with an uncontracted configuration interaction method, and with a CASSCF (622/1) active space built by distributing the eight electrons among nine orbitals (the six valence orbitals plus the three $3p$ orbitals of O).

In an attempt to calibrate our calculations against the results of LAH we carried out CASSCF calculations with the larger (622/1) active space used by these authors. Unfortunately, with the larger ($avqz$) atomic orbital basis the additional three orbitals, which are O $3p$ orbitals in linear geometry, became $3d$ orbitals in perpendicular geometry. This difficulty did not occur in our calculations with the smaller ($avtz$) basis.

Figure 1 compares our calculated $O(^3P)H_2$ PES's with those of LAH, for both colinear and perpendicular geometries. In both geometries, their calculations yield a substantially deeper well. This may be a consequence of the different CI method used. Since our MRCI+Q curves, determined with a larger basis set (with g functions on O and f functions on H), which presumably allows a more complete recovery of the correlation energy, agree quite well with the UCCSD(T) curves, and since the latter method includes an explicit calculation of the effect of triple excitations, we conclude that the calculations of LAH[8] have likely overestimated the binding in the $O(^3P)\cdots H_2$ complex.

In order to resolve this difference we carried out additional CASSCF and MRCI calculations in collinear geometry, where the largest discrepancy with the calculations of LAH occurs (Fig. 1). We used both the $avtz$ and $avqz$ basis sets, and several choices of active space (511/2 and 622/1) in the CASSCF calculations. Further, calculations were done with and without the use of state averaging in the determination of the molecular orbitals. The dissociation energies and minimum O–H_2 distances predicted by these calculations are summarized in Table II. We see little variation among the results of our calculations, and,further, observe that the MRCI+Q dissociation energies agree extremely well with the UCCSD(T) predictions. By contrast, the dissociation energies predicted by LAH[8] are significantly larger.

Li, Apkarian, and Harding give few details on the method they used to determine the diabatic→adiabatic transformation. Consequently, for the lower-symmetry geometries, it was not possible to compare directly our estimate of the diabatic coupling potential-energy surface with theirs.

TABLE II. Calculated values of R_e and D_e for colinear approach of O(^3P) to H_2.[a]

Basis set[b]	Active space	Method	State averaging	R_e (bohr)	D_e (cm^{-1})
				$^3\Pi$ state	
avtz	511/2	MRCI+Q	yes[c]	6.54	12.7
	622/1	MRCI+Q	yes[c]	6.56	12.1
	511/2	MRCI+Q	none[d]	6.58	14.7
		UCCSD(T)	none[e]	6.49	13.8
avqz	511/2	MRCI+Q	yes[c]	6.49	14.3
	511/2	MRCI+Q	none[d]	6.55	13.7
	511/2	MRCI+Q[f]	none[f]	6.39	44.7
				$^3\Sigma^-$ state	
avtz	511/2	MRCI+Q	yes[c]	6.45	67.1
	622/1	MRCI+Q	yes[c]	6.41	69.2
	511/2	MRCI+Q	none[d]	6.41	77.0
		UCCSD(T)	none[e]	6.42	69.8
	622/1	MRCI+Q[f]	none[f]	6.18	108.3
avqz	511/2	MRCI+Q	yes[c]	6.42	67.9
	511/2	MRCI+Q	none[d]	6.41	75.1
	622/1	MRCI+Q[f]	none[f]	6.42	103.1

[a]Internally contracted, configuration interaction calculations, unless specified.
[b]Augmented correlation-consistent bases of Dunning and co-workers (Refs. 17 and 18).
[c]Equal weights assigned to the $^3\Pi$ states (each Cartesian component) and the $^3\Sigma^-$ state in determination of CASSCF orbitals.
[d]CASSCF orbitals determined separately for either the $^3\Pi$ state or the $^3\Sigma^-$ state.
[e]RHF (restricted Hartree-Fock) orbitals determined separately for either the $^3\Pi$ state or the $^3\Sigma^-$ state.
[f]CASSCF and uncontracted configuration interaction calculations done separately for each of the two states (Ref. 8 and *L*. Harding, private communication, 1997).

III. VIBRATIONAL WAVE FUNCTIONS OF THE O(^3P)H_2 COMPLEX

A. Expansion of the PES's

In our previous investigation of the B(^2P)H_2 system,[9] we expressed the interaction potential in a diabatic basis defined by the orientation of the Cartesian $2p$ orbitals of the B atom with the H_2 molecule lying in the xz plane. A similar approach can be made here in terms of the three defined (P_{x^2}, P_{y^2}, P_{z^2}) orbital occupations. There exist three diagonal PES's—$V_{x^2}(R,r,\theta)$, $V_{y^2}(R,r,\theta)$, and $V_{z^2}(R,r,\theta)$. The two orbital occupations of A'' symmetry, which define the diabatic basis, are mixed, except in linear and perpendicular geometry. This mixing is described by an additional potential-energy function, which we denote $V_{xz}(R,r,\theta)$. Finally, it is more appropriate to use the sum and difference of the V_{x^2} and V_{y^2} PES's, which we denote as $V_s(R,r,\theta)$ and $V_d(R,r,\theta)$, which are defined by[9]

$$V_{y^2} = V_s + V_d \tag{9a}$$

and

$$V_{x^2} = V_s - V_d\,. \tag{9b}$$

For notational simplicity, in what follows we shall suppress the dependence on the H_2 bond distance r unless explicitly necessary.

The angular dependence of these PES's can be expanded in terms of reduced rotation matrix elements,[31] or equivalently, regular and associated Legendre polynomials, as follows:

$$V_{z^2}(R,\theta) = \sum_{\lambda=0} V_\lambda^{zz}(R) d_{00}^\lambda(\theta), \tag{10a}$$

$$V_s(R,\theta) = \sum_{\lambda=0} V_\lambda^{s}(R) d_{00}^\lambda(\theta), \tag{10b}$$

$$V_{xz}(R,\theta) = \sum_{\lambda=1} V_\lambda^{xz}(R) d_{10}^\lambda(\theta), \tag{10c}$$

and

$$V_d(R,\theta) = \sum_{\lambda=2} V_\lambda^{d}(R) d_{20}^\lambda(\theta). \tag{10d}$$

For interactions involving a homonuclear diatomic, only the even-λ terms are nonvanishing.[9]

To determine the bound bend–stretch states of the O(^3P)H_2 complex, we follow an important paper by Dubernet and Hutson (DH).[13] Extending earlier work of Launay and Flower,[32,33] DH described several general expansions for the nuclear-electronic wave function describing the interaction of an open-shell atom with a closed-shell molecule, and then derived explicit formulae for the matrix elements of the interaction potential in these bases. In addition, DH explored several decoupling schemes defined by the neglect of various off-diagonal matrix elements.

The interaction potential can be expanded in either a space-fixed (SF) or body-fixed (BF) frame. Adopting, wherever possible, the notation of DH, we write the BF expansion as

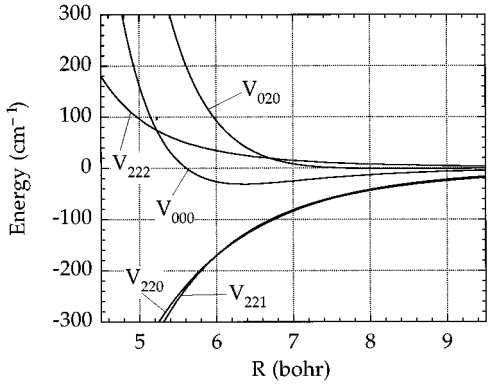

FIG. 4. Dependence on R of the significant $V_{\lambda_r\lambda_a\mu}$ coefficients in the body-frame expansion of the $O(^3P)H_2$ interaction potential [Eq. (11)].

$$V(R,\theta,\phi,\theta_a,\phi_a)$$

$$=\sum_{\lambda_r\lambda_a\mu} V_{\lambda_r\lambda_a\mu}(R)C_{\lambda_a-\mu}(\theta_a,\phi_a)C_{\lambda_r\mu}(\theta,\phi), \tag{11}$$

where $C_{\lambda\mu}$ is an unnormalized spherical harmonic,[31] and $\{\theta_a,\phi_a\}$ represent, collectively, the orientation of the $2p$ orbitals of the O atom (in either the P_{x^2}, P_{y^2}, or P_{z^2} orbital occupations) with respect to R. The index μ is restricted to $0\leqslant\mu\leqslant\min(\lambda_a,\lambda_r)$. For interactions involving an atom with a $p^4(^3P)$ electron occupancy, only the terms with $\lambda_a=0$ and 2 are nonvanishing. Again, for notational simplicity, we have suppressed the dependence on r of the potential and the $V_{\lambda_r\lambda_a\mu}$ expansion coefficients.

The relationship between these $V_{\lambda_r\lambda_a\mu}$ expansion coefficients and the Cartesian based expansion coefficients [Eq. (10)] is given by[10]

$$V_{\lambda_r00}(R)=[2V^s_{\lambda_r}(R)+V^{zz}_{\lambda_r}(R)]/3, \tag{12a}$$

$$V_{\lambda_r20}(R)=5[V^{zz}_{\lambda_r}(R)-V^s_{\lambda_r}(R)]/3, \tag{12b}$$

$$V_{\lambda_r21}(R)=5V^{xz}_{\lambda_r}(R)/\sqrt{6}, \tag{12c}$$

and

$$V_{\lambda_r22}(R)=5V^d_{\lambda_r}(R)/\sqrt{6}. \tag{12d}$$

Again, for interactions involving a homonuclear diatomic, only the λ_r even terms are nonvanishing.

For $O(^3P)H_2$ Fig. 4 displays the variation with R of the most important of the $V_{\lambda_r\lambda_a\mu}$ expansion coefficients. The V_{λ_r00} terms describe the interaction between H_2 and O, averaged over the three orbital occupations. The anisotropy of this average interaction with respect to the rotation of the H_2 molecule is expressed by the V_{λ_r00} terms with $\lambda_r\neq0$. These are very small, and not shown in Fig. 4. The V_{λ_r20} terms describes the difference between the interaction when the doubly filled $2p$ orbital is pointed parallel, as compared to perpendicular, to **R**. We observe in Fig. 4 that of all the anisotropic terms (those with a nonzero value for at least one of the $\lambda_r\lambda_a\mu$ coefficients), the V_{020} term, which expresses the variation of the PES's with the orientation of the O $2p^4$ orbital occupations, averaged over the orientation of the H_2 moiety, and the V_{220} term, which expression the anisotropy in the coupling between the orientational dependence of the O orbital occupations and the rotation of the H_2 moiety, are both significant.

The V_{221} term is also large. This is proportional to the coupling between the P_{x^2} and P_{z^2} configurations induced by approach of the H_2. Finally, the V_{222} term describes the difference in the interaction between the two possible configurations P_{x^2} and P_{y^2} in which the singlet-coupled pair of $2p$ electrons lies perpendicular to **R**.

Alternatively, as discussed by DH, one can expand the interaction potential in a SF basis, with expansion indices λ_r, λ_a, and λ_{12}. The relationship between the SF expansion coefficients, designated $V^{\lambda_r\lambda_a\lambda_{12}}(R)$ and the BF expansion coefficients, defined by Eq. (8), is given by

$$V^{\lambda_r\lambda_a\lambda_{12}}(R)=\sum_\mu (\lambda_r\mu\lambda_a-\mu|\lambda_{12}0)V_{\lambda_r\lambda_a\mu}(R), \tag{13}$$

where $(\cdots\cdot|\cdot\cdot)$ is a Clebsch–Gordan coefficient.[31] It is the body-frame coefficients which provide the most physical insight into the interaction.

B. Full (close-coupled) expansion of the wave function

In the full, or close-coupled (CC), treatment the wave function describing the nuclear motion of the $O(^3P)H_2$ complex is developed by vector coupling the total electronic angular momentum of the atom $\mathbf{j}_a$ with that of the molecule **j** to form $\mathbf{j}_{12}$, which is then coupled with the orbital angular momentum of the O–H_2 pair **L** to form the total angular momentum **J**. The explicit expressions for the internal state wave functions are identical to those given earlier[10] for $B(^2P)H_2$ and for brevity will not be repeated here. The expansion coefficients satisfy the CC equations, which are (in matrix form)

$$\left\{\frac{d^2}{dR^2}\mathbf{1}+\frac{2\mu}{\hbar^2}\left[E\mathbf{1}-\mathbf{V}(R)-\boldsymbol{\epsilon}\right\}\mathbf{C}^J(R)=0, \right. \tag{14}$$

where **1** is the unit matrix, E is the total energy, $\boldsymbol{\epsilon}$ is the diagonal matrix of the internal (spin–orbit and rotational) energies of the separated $O(^3P)+H_2$ states, and $\mathbf{V}(R)$ is the matrix of the interaction potential, which includes centrifugal (rotational) terms as well as the electrostatic interaction, and which goes to zero asymptotically. To determine the matrix elements of the interaction potential, it is most convenient to use the SF expansion of the potential. Explicit expressions for these matrix elements have been given previously by DH [see Eq. (17) of Ref. 13].

C. Body-frame and centrifugal-decoupled expansions of the wave function

Alternatively, it is possible to use a number of different BF expansions of the wave functions. The matrix of the interaction potential is diagonal in P, which is the projection of the total angular momentum along **R**.[13]

By contrast, however, the matrix of the orbital angular momentum **L** is no longer diagonal in a BF expansion. In

general, however, the matrix elements of **L** which couple different values of P, are proportional to J.[13] Under conditions where a weakly bound complex is formed in a supersonic expansion, only low values of J will be populated. It is then often reasonable to neglect the off-diagonal matrix elements of **L**. This defines the so-called centrifugal decoupling (CD) approximation.

Using either a BF, CD-BF, or SF expansion of the wave function, we can obtain the energies and eigenfunctions of the bound states of the $O(^3P)\cdots H_2$ complex by determination of the $C^J(R)$ expansion coefficients in Eq. (14). This can be done either variationally or by numerical solution of the CC equations.

D. Adiabatic bender approximation

Considerable qualitative insight can be obtained by examination of the adiabatic potentials associated with the eigenvalues $w^{ad}(R)$ of the Hamiltonian exclusive of the R-dependent kinetic-energy term.[34–37] These are defined by

$$\mathbf{w}^{ad}(R)=\mathbf{T}(R)[\mathbf{V}(R)+\boldsymbol{\epsilon}]\mathbf{T}(R)^T, \tag{15}$$

where $\mathbf{T}(R)$ is the matrix which diagonalizes $\mathbf{V}(R)+\boldsymbol{\epsilon}$ at each value of R. Since the BF and SF expansion states are related by an orthogonal transformation,[38] the locally adiabatic states are identical whether the Hamiltonian is constructed in a BF or SF basis.

Within the CD approximation, the $\mathbf{V}(R)$ matrix, exclusive of centrifugal terms, is block diagonal in P and independent of the sign of P.[13,39,40] In this case, additional physical insight can be gained by an examination of the definite-P adiabatic energies, obtained by diagonalization of the block of the BF $\mathbf{V}(R)+\boldsymbol{\epsilon}$ matrix which corresponds to the chosen value of P.

Figure 5 displays the radial adiabatic bender potentials for $O(^3P)pH_2$ (upper panel) and $O(^3P)oH_2$ (lower panel). Each of the three spin–orbit states of O gives rise to an attractive potential. In the case of the interaction with pH_2 the interpretation of the curves is particularly simple. For a spherical partner ($j=0$) within the centrifugal decoupling approximation the on-block elements of the potential matrix reduce to

$$\mathbf{V}(R)=V_{000}(R)\mathbf{1}+\frac{\hbar^2}{2\mu R^2}J(J+1)+\mathbf{V}_P(R), \tag{16}$$

where the matrix $\mathbf{V}_P(R)$ is given by the following expressions:

for $P=0$

$j_a\backslash j_a'$	0	1	2
0	0	0	$-2^{1/2}V_{020}/5$
1	0	$-0.2V_{020}+1/\mu R^2$	0
2	$-2^{1/2}V_{020}/5$	0	$0.2V_{020}+3/\mu R^2$

(17)

for $P=1$

$j_a\backslash j_a'$	1	2
1	$0.1V_{020}$	$-0.3V_{020}$
2	$-0.3V_{020}$	$0.1V_{020}+2/\mu R^2$

(18)

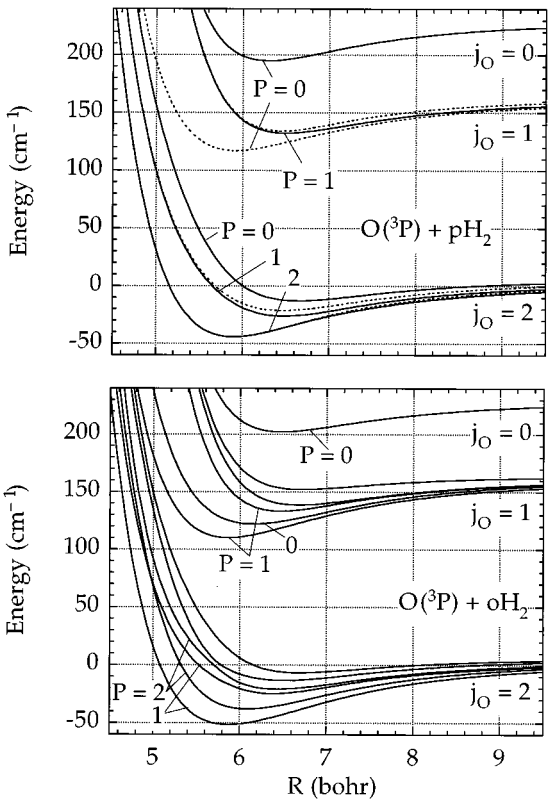

FIG. 5. Dependence on R of the lower (attractive) adiabatic bender potentials for $O(^3P)pH_2$ (upper panel) and $O(^3P)oH_2$ (lower panel) for a total angular momentum of $J=2$. The solid curves correspond to e-labeled states ($+$ total parity for $J=2$), and the dashed curves, to f-labeled states ($-$ total parity for $J=2$). The splitting between the solid and dashed curves, for a nominal value of P and j_O, is the parity splitting discussed in Sec. IV. Similar adiabatic bender calculations, within the CD approximation, have been used to provide the P-labeling, which is indicated for all the curves in the upper panel and the lower members of each of the three multiplet clumps in the lower panel.

and, for $P=2$

$j_a\backslash j_a'$	2
2	$-0.2V_{020}-2/\mu R^2$

(19)

Here, V_{000} and V_{020} designate two of the R-dependent body-frame expansion coefficients discussed earlier in Sec. III A and displayed in Fig. 4.

In particular, in the analogous interaction of a noble gas with $O(^3P)$,[42] V_{020} is, from Eq. (12b), proportional to $V_\Sigma - V_\Pi$. The $V_{020}(R)$ term is positive, because in the Σ^- orientation two of the oxygen $2p$ electrons are pointing directly toward the partner, rather than only one in the Π orientation. Hence, from Eqs. (17)–(19), we predict that the $j=2$, $P=2$ level will have the most attractive potential, as can be seen in Fig. 5. We further see that the $P=1$ levels of both $j=1$ and $j=2$ have identical diagonal potentials and should show roughly equivalent shapes, as is apparent in Fig. 5.

In complexes formed with an atom in a ^2P electronic state, the splitting between the lower two bender curves at the molecular minimum is quenched to $\sim 2/3$ of the atomic value.[43,44] In the present case, a complex with an atom in a $p^4(^3P)$ electronic state, Eqs. (17)–(19) reveal that the splitting between the lowest $j=2$ and $j=1$ bender curves at the molecular minimum is actually larger, by $0.3\ V_{020}$, than the

TABLE III. Energies (cm^{-1}) of lower bend–stretch levels of the $O(^3P)$ complex.

Method[a]	$P=0(J=0)$[b]	$P=1(J=1)$[b]	$P=2(J=2)$[b]
		pH_2	
CD	−4.02	−5.50	−14.73
CC *e*	−4.02	−7.33	−15.39
CC *f*	...[c]	−5.53	−15.31
		oD_2	
CD	−9.72	−11.81	−23.07
CC *e*	−9.72	−12.66	−23.27
CC *f*	...[c]	−11.81	−23.26
		oH_2	
CD	−9.45	−21.95	−12.69
CC *e*	−6.13	−22.36	−12.29
CC *f*	−9.45	−22.40	−12.49
		pD_2	
CD	−17.59	−31.23	−19.94
CC *e*	−12.16	−31.36	−19.83
CC *f*	−17.59	−31.34	−19.85

[a]The *e* and *f* labels refer, respectively, to levels of total parity $(-1)^J$ and $-(-1)^J$.
[b]The three columns correspond to the lowest values of J allowed for each P.
[c]Only *e*-labeled bound states exist for the $P=0$ levels of the even-j nuclear spin isomers.

asymptotic splitting between these fine-structure states.

In the exact (CC) formulation, states of overall even or odd parity, which correspond to the two possible linear combinations of the $\pm P$ BF projection states, are split. This splitting can be observed clearly in the adiabatic bender potential curves shown in Fig. 5, particularly for the curves which correlate to the $j_O=1$ level.

The lower panel of Fig. 5 displays the radial adiabatic bender potentials for $O(^3P)oH_2$. The threefold rotational degeneracy of the H_2 molecule in $j=1$ along with the fivefold degeneracy of the lowest spin–orbit state of O renders more complex the relatively simple structure of the pH_2 adiabatic bender potentials (Fig. 5 upper panel). In particular, the coupling between the three internal angular momenta (j_a, j, and L) gives rise to a complex avoided crossing among all but the lowest of the $O(^3P)oH_2$ adiabatic bender potentials which correlate with the lowest spin–orbit state of the separated products $[O(^3P_2)+H_2(j=1)]$.

IV. BEND–STRETCH LEVELS OF THE $O(^3P)H_2$ COMPLEX

We subsequently carried out variational determinations of the $O(^3P)H_2$ bend–stretch energies, within the CC and CD descriptions. We used the distributed Gaussian method of Hamilton and Light.[45] Table III lists the energies [relative to $H_2+O(^3P_2)$] of the complexes involving the even-j nuclear spin isomers of hydrogen (pH_2 and oD_2). As we anticipate from the adiabatic bender curves in Fig. 5, the lowest state corresponds to $P=2$. Furthermore, because of the increase in reduced mass, the deuterium complexes are significantly more strongly bound.

The energies of the lowest vibrational levels of complexes of $O(^3P)$ with the odd-j nuclear spin isomers (oH_2 and pD_2) are also listed in Table III. In contrast to the case of $j=0$, in $j=1$ the molecule can orient itself and thus more efficiently sample to the more attractive regions of the potential. For this reason the dissociation energies are larger for the odd-j isomers. However, as we have seen in the analysis of the oH_2 adiabatic bender curves (lower panel of Fig. 5), the coupling between the orientation of the H_2 axis and the orientation of the O $2p$ electrons is obscured by the presence of the strong spin–orbit coupling.

TABLE IV. Dissociation energies (cm^{-1}) of lowest level of complexes of $O(^3P)$ with H_2.

Ligand	Full CC	Free rotor[a]
pH_2	15.4	14.0
oH_2	22.4	22.0
oD_2	22.3	20.7
pD_2	31.4	31.0

[a]Only the $j=0$ level (for pH_2 and oD_2) or only the $j=1$ level (for oH_2 or pD_2) included in the rotational basis.

For pH_2 in its lowest rotational level ($j=0$), if coupling to higher rotational levels are ignored, then only the $V_{\lambda_r\lambda_a\mu}$ terms with $\lambda_r=0$ will be nonvanishing. As can be seen in Fig. 4, and from our discussion earlier in this paper, V_{020} is positive, which implies that the anisotropy in the $O(^3P)H_2$ potential will preferentially orient the O atom with respect to the nearly spherical pH_2 so that the singlet-coupled, doubly filled p orbital is pointed perpendicular to R. For pH_2 in its lowest rotational level ($j=0$), the H_2 molecule behaves as a sphere, which itself cannot be oriented. Notwithstanding, if the anisotropy is large enough, higher rotational levels of pH_2 ($j=2,4,...$) will contribute to the total wave function, and hence lead to some degree of orientation. Because the rotational spacing of the H_2 molecule is so large ($B_e=60.85\ cm^{-1}$ [46]), the contribution of the higher rotational levels will be small.

In the calculations summarized in Table III, successively higher rotational levels of H_2 were added to the basis until the calculated energies were converged within $0.05\ cm^{-1}$. Table IV compares the zero-point corrected dissociation energies of the most strongly bound of the states of each complex with those calculated with only the $j=0$ level included in the rotational basis. We see that the addition of the $j=2$ (and higher) rotational levels to the basis increases the binding energy of the lowest vibrational levels of the complexes with pH_2 and oD_2 by less than 5%, compared to what might be denoted a ''free rotation'' model, in which only the $j=0$ levels of H_2 were included. Clearly, then, for the even nuclear spin-isomers, the H_2 molecule behaves as a spherical entity in the complex.

Similarly, in the case of complexes with the odd-j nuclear spin isomers, we see in Table IV that the addition of $j=3$ (and higher) rotational levels in the expansion of the wave function has only a small effect on the calculated dissociation energies of the lowest vibrational level of the complex. Thus, the rotation of these odd-j nuclear spin isomers is not quenched in the complex.

As discussed at the end of Sec. III, in the exact (CC) treatment, the even and odd parity levels, which correspond to the two possible linear combinations of the $\pm P$ BF projection states, are split. In analogy with the convention in

diatomic molecule spectroscopy,[43,47] we use the label e to identify states whose parity is equal to $(-1)^J$ and the label f to identify states whose parity is equal to $-(-1)^J$. The parity splitting is here analogous to the Λ-doubling in a diatomic molecule in a $^3\Pi$ electronic state (indeed, it is equivalent for colinear geometries). For a diatomic molecule in a $^3\Pi$ electronic state, theΛ-doublet splitting is largest for the $^3\Pi_0$ levels ($P=0$), significant also for the $^3\Pi_1$ levels, but very small for the $^3\Pi_2$ levels ($P=2$).[48]

Similar qualitative behavior is seen in the complexes of $O(^3P)$ with H_2. For the complexes with even-j hydrogen, only the e-labeled $P=0$ states support bound vibrational levels. For the complexes with odd-j hydrogen, both e and f-labeled bound states exist for all values of P. We observe in Table III that the splittings are indeed largest for $P=0$, but negligible for $P=2$.

Several authors[36,49] have used perturbation theory to analyze the parity splittings in weakly bound complexes involving atoms in ^2P electronic states.[50] A similar analysis could be carried out here, should there be eventual spectroscopic interest.

Because of the light reduced mass (1.70 amu for $O+H_2$), the centrifugal barrier is significant, even at low values of J. From the adiabatic bender curves in Fig. 5 it is easy to extract an excellent approximation to the rotational constant. One uses these curves in a simple one-dimensional Hamiltonian to obtain a vibrational wave function, from which one can evaluate the rotational constant as $B=\langle R^{-2}\rangle/2\mu$. We predict $B=0.750$ and $0.785\ \mathrm{cm}^{-1}$, respectively, for the lowest bend–stretch levels of $O(^3P)pH_2$ and $O(^3P)oH_2$.

V. CONCLUSION

In this paper we have presented a complete *ab initio* study of complexes of O in its ground (^3P) electronic state with both H_2 and D_2. Our investigation involved a determination of the relevant potential-energy surfaces in the region of the van der Waals minima, including, specifically, the diabatic→adiabatic transformation between the two possible electronic configurations of the O atom which are both antisymmetric with respect to the triatomic plane [$p_x^2p_yp_z$ and $p_xp_yp_z^2$]. With these potential-energy surfaces, we carried out an essentially exact determination of the bend–stretch eigenstates of the binary $O(^3P)\cdots H_2$ complex, including, specifically, the spin–orbit coupling in the O atom.

The predicted dissociation energies (D_0) are 15.4 and $22.4\ \mathrm{cm}^{-1}$ for the complexes with pH_2 and oD_2, respectively. In these complexes the hydrogen moiety (in $j=0$) behaves essentially as a spherical entity. In the complexes with oH_2 and pD_2, in which the directionality of the rotational motion ($j=1$) allows the molecule to orient itself with respect to the $O–H_2$ axis, the dissociation energy is enhanced by $\sim 10\ \mathrm{cm}^{-1}$ ($D_0=22.4$ and $31.4\ \mathrm{cm}^{-1}$ for oH_2 and pD_2, respectively). In both cases, however, our estimate of the dissociation energy is substantially less than the earlier estimate by Li, Apkarian, and Harding.[8] [$D_0\sim 50\ \mathrm{cm}^{-1}$ for $O(^3P)\cdots H_2$]. This is a consequence of both the deeper potentials reported by these authors (see Fig. 1) and, possibly, of their more approximate treatments of the diabatic coupling and the nuclear motion in the complex.

We predict the dissociation energy of the $O(^3P)\cdots H_2$ complex to be only half of that of the comparable $B(^2P)\cdots H_2$ complex (22.4 as compared to $48.5\ \mathrm{cm}^{-1}$ [10] for the more favorable case of oH_2). Even in the most attractive orientation, in the $O(^3P)\cdots H_2$ complex there remains a singly occupied O $2p$ orbital pointing in the direction of the H_2 ligand. This reduces, by Pauli repulsion, the magnitude of the dispersion interaction. The $B(^2P)$ atom, in contrast, has only one $2p$ electron, which can be assigned to an orbital which is perpendicular to the $B–H_2$ axis.

The complex with oH_2 is predicted to be $\sim 10\ \mathrm{cm}^{-1}$ more strongly bound than the complex with pH_2. This, coupled with the enhanced statistical abundance of oH_2 (3:1), implies that preparation of $O(^3P)H_2$ complexes in a supersonic expansion of nH_2 will give rise primarily to complexes involving oH_2. The first-order rate constant for ortho→para conversion in pure H_2 is very small ($\sim 10^{-2}\ \mathrm{h}^{-1}$ [51]). The presence of an open-shell atom is expected to increase the conversion rate constant dramatically ($k=10^2–10^3\ \mathrm{h}^{-1}$).[52] Notwithstanding, this conversion will be extremely slow on the time scale of a typical molecular beam experiment.

Despite the relatively small predicted dissociation energy, as compared to $B(^2P)\cdots H_2$, the dissociation energies are comparable to those for $B(^2P)\cdots Ne$ and $OH(X\ ^2\Pi)\cdots Ne$, both of which have been seen experimentally by means of optical spectroscopy.[27,53–56] Consequently, we are hopeful that the present study will encourage future experimental investigations of the $O(^3P)\cdots H_2$ complex. Our work can serve as a guide to the interpretation of these difficult experiments, as it did in the case of the $B(^2P)\cdots H_2$ complex.[10,11]

Finally, the potential-energy surfaces determined here can be used to model the potentials for complexes of $O(^3P)$ with multiple H_2 ligands. This would allow, for example, classical dynamical simulations, of the kind reported by Li *et al.*[8] or quantum diffusion Monte Carlo studies, such as we have done for $B(^2P)(pH_2)_n$.[57]

Note added in proof. Dobby and Knowles [A. J. Dobbyn and P. J. Knowles, Mol. Phys. **91**, 1107 (1997)] have reported a similar success in using matrix elements of the orbital angular momentum to obtain the adiabatic → diabatic transformation in the region of the $^1\Sigma^+/^1\Pi$ conical intersection of the $O(^1D)H_2$ states.

ACKNOWLEDGMENTS

The author is grateful to the U.S. Air Force Office of Scientific Research for support of the research reported here, under grants No. F49620-95-1-0055, F49620-95-1-0099, and F49620-98-1-0187. He would also like to thank Paul Dagdigian for his continued encouragement and helpful discussions, and Larry Harding for incisive comments on the original manuscript. Part of this work was accomplished while Millard Alexander was on sabbatical leave at the Physical and Theoretical Chemistry Laboratory at the University of Oxford. He is grateful for the support of a John Simon Guggenheim Memorial Fellowship and a Dr. Lee's Visiting Fellowship from Christ Church, Oxford.

[1] J. Warnatz, in *Combustion Chemistry*, edited by J. W. C. Gardiner (Springer-Verlag, New York, 1984), p. 97.
[2] R. E. Howard, A. D. McLean, and W. A. Lester, Jr., J. Chem. Phys. **71**, 2412 (1979).
[3] G. C. Schatz, A. F. Wagner, S. P. Walch, and J. M. Bowman, J. Chem. Phys. **74**, 4984 (1981), T. T. Lee, J. M. Bowman, A. F. Wagner, and G. C. Schatz, *ibid.* **76**, 3563 (1982); **76**, 3583 (1982); J. M. Bowman, A. F. Wagner, S. P. Walch, and T. H. Dunning, Jr., *ibid.* **81**, 1739 (1984); J. M. Bowman and A. F. Wagner, *ibid.* **86**, 1967 (1987); A. F. Wagner and J. M. Bowman, *ibid.* **86**, 1976 (1987).
[4] A. F. Wagner, J. M. Bowman, and L. B. Harding, J. Chem. Phys. **82**, 1866 (1985).
[5] B. C. Garrett, D. G. Truhlar, J. M. Bowman, and A. F. Wagner, J. Phys. Chem. **90**, 4305 (1986).
[6] M. H. Alexander (unpublished).
[7] S. P. Walch, T. H. Dunning, Jr., F. W. Bobrowicz, and R. C. Raffenetti, J. Chem. Phys. **72**, 406 (1980).
[8] Z. Li, V. A. Apkarian, and L. B. Harding, J. Chem. Phys. **106**, 942 (1997).
[9] M. H. Alexander, J. Chem. Phys. **99**, 6014 (1993).
[10] M. H. Alexander and M. Yang, J. Chem. Phys. **103**, 7956 (1995).
[11] X. Yang, E. Hwang, M. H. Alexander, and P. J. Dagdigian, J. Chem. Phys. **103**, 7966 (1995).
[12] F. Rebentrost and W. A. Lester, Jr., J. Chem. Phys. **64**, 3879 (1976).
[13] M.-L. Dubernet and J. M. Hutson, J. Chem. Phys. **101**, 1939 (1994).
[14] F. Rebentrost and W. A. Lester, Jr., J. Chem. Phys. **63**, 3737 (1975).
[15] H.-J. Werner, B. Follmeg, and M. H. Alexander, J. Chem. Phys. **89**, 3139 (1988).
[16] P. J. Knowles and H.-J. Werner, Chem. Phys. Lett. **115**, 259 (1985).
[17] T. H. Dunning, Jr., J. Chem. Phys. **90**, 1007 (1989).
[18] R. A. Kendall, T. H. Dunning, Jr., and R. J. Harrison, J. Chem. Phys. **96**, 6796 (1992).
[19] K. Stark and H.-J. Werner, J. Chem. Phys. **104**, 6515 (1996).
[20] H.-J. Werner and P. J. Knowles, Theor. Chim. Acta **78**, 175 (1990).
[21] E. R. Davidson and D. W. Silver, Chem. Phys. Lett. **53**, 403 (1977).
[22] The Davidson correction used here is defined by $\Delta E = E_{\rm cor}(1-c^2)/c^2$, where $E_{\rm cor}$ is the calculated correlation energy and c is the norm of the internally contracted CI wave function.
[23] MOLPRO is a package of *ab initio* programs written by H.-J. Werner and P. J. Knowles, with contributions from J. Almlöf, R. D. Amos, M. J. O. Deegan, S. T. Elbert, C. Hampel, W. Meyer, K. Peterson, E. A. Reinsch, R. Pitzer, A. Stone, and P. R. Taylor.
[24] P. J. Knowles, C. Hampel, and H.-J. Werner, J. Chem. Phys. **99**, 5219 (1993).
[25] M. Deegan and P. J. Knowles, Chem. Phys. Lett. **227**, 321 (1994).
[26] S. F. Boys and F. Benardi, Mol. Phys. **19**, 553 (1970).
[27] X. Yang, E. Hwang, P. J. Dagdigian, M. Yang, and M. H. Alexander, J. Chem. Phys. **103**, 2779 (1995).
[28] M. Yang, M. H. Alexander, H.-J. Werner, and R. Bemish, J. Chem. Phys. **105**, 10462 (1996).
[29] F. B. Brown and D. G. Truhlar, Chem. Phys. Lett. **117**, 307 (1985).
[30] D. Sölter, H.-J. Werner, M. von Dirke, A. Untch, A. Vegiri, and R. Schinke, J. Chem. Phys. **97**, 3357 (1992).
[31] D. M. Brink and G. R. Satchler, *Angular Momentum*, 2nd ed. (Clarendon, Oxford, 1968).
[32] J. M. Launay, J. Phys. B **10**, 3665 (1977).
[33] D. R. Flower and J. M. Launay, J. Phys. B **10**, 3673 (1977).
[34] S. L. Holmgren, M. Waldman, and W. Klemperer, J. Chem. Phys. **67**, 4414 (1977).
[35] M. H. Alexander, S. Gregurick, and P. J. Dagdigian, J. Chem. Phys. **101**, 2887 (1994).
[36] M. H. Alexander, S. Gregurick, P. J. Dagdigian, G. W. Lemire, M. J. McQuaid, and R. C. Sausa, J. Chem. Phys. **101**, 4547 (1994).
[37] M. Yang, M. H. Alexander, C.-C. Chuang, R. W. Randall, and M. I. Lester, J. Chem. Phys. **103**, 905 (1995).
[38] M. H. Alexander and P. J. Dagdigian, J. Chem. Phys. **101**, 7468 (1994).
[39] M. H. Alexander, J. Chem. Phys. **76**, 5974 (1982).
[40] D. J. Kouri, in *Atom-Molecule Collision Theory: A Guide for the Experimentalist*, edited by R. B. Bernstein (Plenum, New York, 1979), p. 301.
[41] C. E. Moore, *Atomic Energy Levels, NSRDS-NBS 35* (U. S. Government Printing Office, Washington, 1971).
[42] Z. Ma, K. Liu, L. B. Harding, M. Komotos, and G. C. Schatz, J. Chem. Phys. **100**, 8026 (1994).
[43] H. Lefebvre-Brion and R. W. Field, *Perturbations in the Spectra of Diatomic Molecules* (Academic, New York, 1986).
[44] E. Hwang and P. J. Dagdigian, Chem. Phys. Lett. **233**, 483 (1995).
[45] I. P. Hamilton and J. C. Light, J. Chem. Phys. **84**, 306 (1986).
[46] K. P. Huber and G. Herzberg, *Molecular Spectra and Molecular Structure. IV. Constants of Diatomic Molecules* (Van Nostrand Reinhold, New York, 1979).
[47] J. M. Brown, J. T. Hougen, K.-P. Huber, J. W. C. Johns, I. Kopp, H. Lefebvre-Brion, A. J. Merer, D. A. Ramsay, J. Rostas, and R. N. Zare, J. Mol. Spectrosc. **55**, 500 (1975).
[48] G. Herzberg, *Spectra of Diatomic Molecules*, 2nd ed. (Van Nostrand, Princeton, New Jersey, 1968).
[49] W. H. Green, Jr. and M. I. Lester, J. Chem. Phys. **96**, 2573 (1992).
[50] M.-L. Dubernet and J. M. Hutson, J. Phys. Chem. **98**, 5844 (1994).
[51] A. Farkas, *Orthohydrogen, Parahydrogen, and Heavy Hydrogen* (Cambridge University Press, Cambridge, United Kingdom 1935).
[52] E. R. Davidson and D. W. Silver, Chem. Phys. Lett. **52**, 403 (1978).
[53] B.-C. Chang, D. W. Cullin, J. M. Williamson, J. R. Dunlop, B. D. Rehfuss, and T. A. Miller, J. Chem. Phys. **96**, 3476 (1992).
[54] B.-C. Chang, J. R. Dunlop, J. W. Williamson, T. A. Miller, and M. C. Heaven, Chem. Phys. Lett. **207**, 62 (1993).
[55] M. I. Lester, C.-C. Chuang, P. M. Andrews, M. Yang, and M. H. Alexander, Faraday Discuss. Chem. Soc. **102**, 311 (1995).
[56] C.-C. Chuang, P. Andrews, and M. I. Lester, J. Chem. Phys. **103**, 3418 (1995).
[57] A. Vegiri, M. H. Alexander, S. Gregurick, A. McCoy, and R. B. Gerber, J. Chem. Phys. **100**, 2577 (1994).